The EMBO Journal Vol. 19 No. 22 pp. 6020–6029, 2000

Vezatin, a novel transmembrane protein, bridges myosin VIIA to the cadherin–catenins complex

Polonca Küssel-Andermann, Aziz El-Amraoui, Saaid Safieddine, Sylvie Nouaille, Isabelle Perfettini, Marc Lecuit[1], Pascale Cossart[1], Uwe Wolfrum[2] and Christine Petit[3]

Unité de Génétique des Déficits Sensoriels, CNRS URA 1968 and [1]Unité des Interactions Bactéries-Cellules, Institut Pasteur, 25–28 rue du Dr Roux, 75724 Paris cedex 15, France and [2]Zoologisches Institute, Johannes Gütenberg-Universität Mainz, 55099 Mainz, Germany

[3]Corresponding author
e-mail: cpetit@pasteur.fr

P.Küssel-Andermann and A.El-Amraoui contributed equally to this work

Defects in myosin VIIA are responsible for deafness in the human and mouse. The role of this unconventional myosin in the sensory hair cells of the inner ear is not yet understood. Here we show that the C-terminal FERM domain of myosin VIIA binds to a novel transmembrane protein, vezatin, which we identified by a yeast two-hybrid screen. Vezatin is a ubiquitous protein of adherens cell–cell junctions, where it interacts with both myosin VIIA and the cadherin–catenins complex. Its recruitment to adherens junctions implicates the C-terminal region of α-catenin. Taken together, these data suggest that myosin VIIA, anchored by vezatin to the cadherin–catenins complex, creates a tension force between adherens junctions and the actin cytoskeleton that is expected to strengthen cell–cell adhesion. In the inner ear sensory hair cells vezatin is, in addition, concentrated at another membrane–membrane interaction site, namely at the fibrillar links interconnecting the bases of adjacent stereocilia. In myosin VIIA-defective mutants, inactivity of the vezatin–myosin VIIA complex at both sites could account for splaying out of the hair cell stereocilia.

Keywords: catenins/E-cadherin/FERM domain/ myosin VIIA/vezatin

Introduction

Mutations in the genes encoding unconventional myosins VI, VIIA and XV cause hearing loss in man and/or mouse (Avraham *et al*., 1995; Gibson *et al*., 1995; Weil *et al*., 1995; Probst *et al*., 1998; Wang *et al*., 1998). The inner ear sensory hair cells of mice defective for any of these unconventional myosins are characterized by anomalies of their stereocilia (Avraham *et al*., 1995; Gibson *et al*., 1995; Probst *et al*., 1998; Self *et al*., 1998), i.e. stiff apical microvilli that form the hair bundle, the mechanoreceptive structure for sound stimulation. These anomalies differ from one myosin defect to another, indicating different roles for these actin-based motor molecules in the formation and/or organization of the hair bundle. *Myo7a* defective mice (*shaker-1* deaf mutants) (Gibson *et al*., 1995) are characterized by a splaying out of the hair cell stereocilia (Self *et al*., 1998); in addition, uptake of aminoglycosides by the hair cells is impaired (Richardson *et al*., 1997). The same anomalies are observed in *myo7a*$^{-/-}$ zebrafish mutants (*mariner* mutants) (Ernest *et al*., 2000), suggesting that the function of myosin VIIA in the hair cells has been preserved throughout the evolution of vertebrates. In addition to the inner ear hair cells (Hasson *et al*., 1995, 1997; El-Amraoui *et al*., 1996), myosin VIIA is also present in a variety of murine organs or tissues, including the retina, olfactory epithelium, brain, choroid plexus, intestine, liver, kidney, adrenal gland and testis (Sahly *et al*., 1997; Wolfrum *et al*., 1998). However, the phenotypes associated with myosin VIIA mutations in mice and humans have so far only comprised deleterious alterations of the inner ear and the eye (Liu *et al*., 1998, 1999; Self *et al*., 1998). The structure of myosin VIIA is highly conserved in vertebrates and invertebrates (Hoyt *et al*., 1997; Mermall *et al*., 1998; Oliver *et al*., 1999), with a motor head domain containing ATP and actin binding motifs, a neck region composed of five IQ (isoleucine/ glutamine) motifs expected to bind calmodulin and a long tail (1359 amino acids in man). The tail begins with a short coiled-coil domain that, by the yeast two-hybrid system, has been shown to form homodimers (Weil *et al*., 1997). This domain is followed by two large repeats of ~460 amino acids, each containing a MyTH4 (myosin tail homology 4) and a FERM (4.1, ezrin, radixin, moesin)-like domain, separated by a poorly conserved SH3 (src homology type 3) domain (Chen *et al*., 1996; Mermall *et al*., 1998; Oliver *et al*., 1999). The tandem association of MyTH4 and FERM domains also exists in other proteins (Mermall *et al*., 1998; Oliver *et al*., 1999), arguing in favour of a functional significance for this pairing. Moreover, FERM domains have been shown to be involved in membrane attachment, either via binding to phospholipids or through direct interactions with specific transmembrane proteins (Chishti *et al*., 1998). The structural diversity of the tails of unconventional myosins is believed to dictate the specificity of their functions within the cell (Hoyt *et al*., 1997; Mermall *et al*., 1998; Oliver *et al*., 1999). In particular, among the several molecules that are expected to interact with the tail of a given myosin, some are likely to determine the targets to which is applied the force generated by the myosin motor head. In order to obtain an insight into the roles of myosin VIIA, we screened for proteins interacting with its tail using a yeast two-hybrid system (Küssel-Andermann *et al*., 2000) and identified a

Published by Oxford University Press

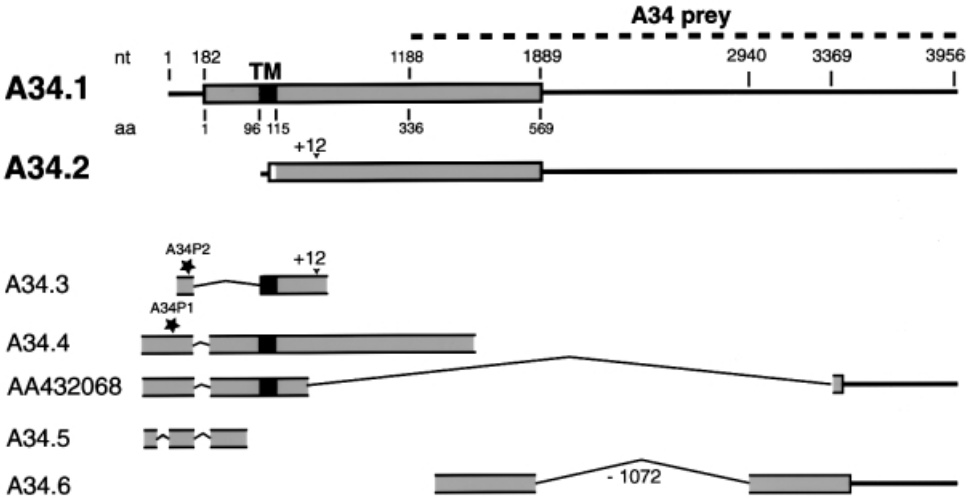

Fig. 1. Schematic representation of vezatin splice variants. For each cDNA the open reading frame (ORF) is represented by a grey box and the putative transmembrane domain (TM), when present, by a black box. The A34 fragment (dashed line) that was identified by the yeast two-hybrid screen is indicated (A34 prey). Two cDNA clones containing complete ORFs, A34.1 and A34.2, were obtained. The A34.1 sequence predicts an ATG initiator codon preceded by a stop codon 18 nt upstream. It encodes a putative 569 amino acid protein, with a transmembrane domain (amino acids 96–115) but no signal peptide. A34.1 is used as a reference for nucleotide and amino acid positions. A34.2 has a distinct predicted ATG initiator codon preceded by a stop codon 6 nt upstream. The deduced 460 amino acid protein sequence lacks the TM segment; it differs from the A34.1 sequence by the N-terminal 10 amino acids. These two cDNAs were also present in a human retinal library. In addition, partial cDNA sequences were obtained. A34.3 and A34.5 cDNAs, which were obtained by 5′-RACE, contain short in-frame deletions (339 nt in A34.3 and two deletions of 57 and 73 nt in A34.5) in the extracellular region. A34.4, A34.5 and EST AA432068 carry a 73 nt deletion (nt 134–206) encompassing the ATG initiator codon of A34.1, thus resulting in an upstream extension of the ORF. In A34.2 and A34.3 cDNAs a 12 nt in-frame insertion (+12) at nt position 749 (amino acid 249) was observed. In A34.6 and several ESTs (see Materials and methods) a 1072 nt deletion (–1072), covering nt 1869–2940 of A34.1, results in an ORF extension of 182 amino acids into the 3′-untranslated region. Finally, EST AA432068 encodes a putative vezatin variant with a short cytoplasmic tail, which lacks the myosin VIIA interacting domain (nt 1188–1889). Stars indicate the positions of the two human peptides, A34P1 and A34P2, used to generate antibodies.

novel transmembrane protein of adherens cell junctions, which we named vezatin.

Results

Identification of vezatin, a novel transmembrane protein interacting with the C-terminal FERM domain of myosin VIIA

The C-terminal region of myosin VIIA, corresponding to the MyTH4 and FERM domains (i.e. the last 464 amino acids), was used as the bait in the yeast two-hybrid system. Since myosin VIIA is expressed in the retina (Hasson *et al*., 1995; El-Amraoui *et al*., 1996; Liu *et al*., 1997), a yeast two-hybrid library expressing human retinal proteins fused with the GAL4 transcriptional activating domain was screened (Küssel-Andermann *et al*., 2000). A first prey composed of 234 amino acids encoded by clone A34 was considered to be a myosin VIIA specific ligand as no interaction could be observed with two control proteins, namely lamin C and merlin/schwannomin, which also possess a FERM domain (data not shown). A longer cDNA clone, A34.1 (DDBJ/EMBL/GenBank accession No. AF216644), containing an entire open reading frame (Figure 1), was subsequently isolated from a human retinal cDNA library (see Materials and methods). The deduced amino acid sequence predicted a 569 amino acid protein (mol. wt 65.4 kDa) with a single putative transmembrane domain (amino acids 96–115) and a potential C-terminal intracytoplasmic region of 454 amino acids (von Heijne and Gavel, 1988; Rost *et al*., 1995). This protein showed no similarity with any known protein and was named vezatin (derived from Slovenian *vezati* = bind, connect) based on functional considerations (see below). Comparison of the sequences of additional cDNA clones, 5′-RACE–PCR products and ESTs (see Materials and methods) with available human genome sequences demonstrated the existence of multiple vezatin splice variants (Figure 1). None of these sequences extended upstream of that of A34.4 (see Figure 1 and Materials and methods). One of the other cDNA clones isolated, A34.2 (DDBJ/EMBL/GenBank accession No. AF277625), also contained an entire open reading frame with a distinct ATG initiator codon and coded for a predicted protein with no transmembrane domain (Figure 1).

We generated polyclonal antibodies against the C-terminal region of vezatin (see Materials and methods). In line with the variety of predicted isoforms (see Figure 1), immunoblot analysis of murine tissues (inner ear, retina, brain, lung, kidney and heart) showed several bands, with two major ones of ~125 and 90 kDa (Figure 2A). In the various epithelial (Caco-2, LLCPK, MDCK, HEK293 and HeLa) and non-epithelial (NIH 3T3 and PC12) cell lines tested two predominant bands of 125 and 90 kDa were also detected (data not shown). These two bands were also detected by antibodies generated against two peptides from the predicted extracytoplasmic N-terminal region (see Materials and methods and Figure 1) (data not shown).

To confirm the interaction of myosin VIIA with vezatin, the mammalian cell line HEK293 was co-transfected with plasmids encoding the myosin VIIA tail (amino acids 848–2215) and A34.2 (460 amino acids) tagged with myc (see Materials and methods). Cell extracts were incubated with either anti-myosin VIIA or anti-myc antibodies.

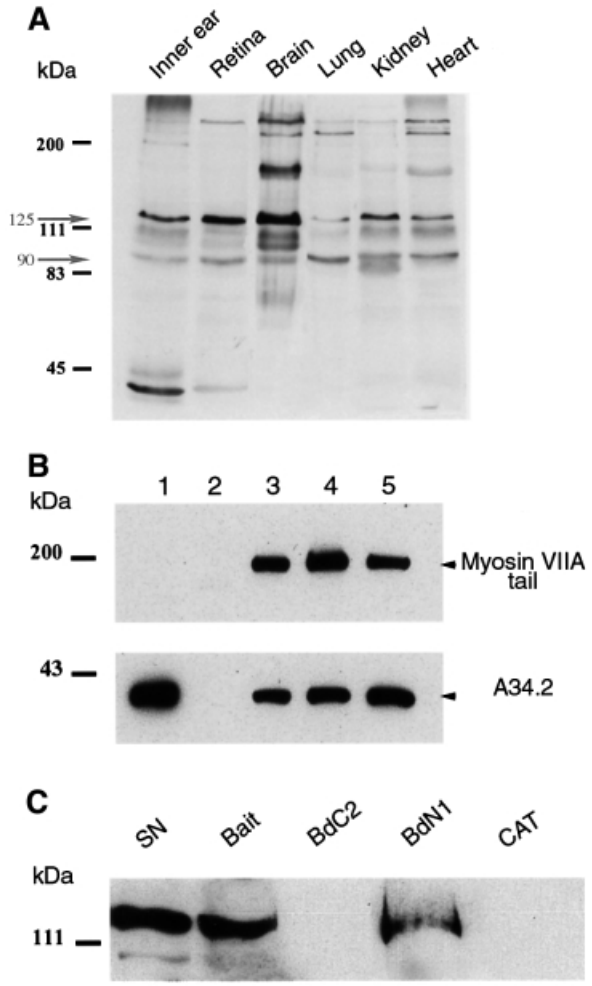

Fig. 2. Vezatin binds to the C-terminal FERM domain of myosin VIIA. (**A**) Expression of vezatin in adult mouse tissues. Total protein extracts (10 μg/lane) from six different tissues of 10-day-old mice were immunoblotted with the anti-mA34 antibody. Multiple vezatin isoforms are observed in all tissues. The higher bands may correspond to vezatin isoforms with large extracellular domains (see Figure 1). (**B**) Binding of vezatin to the myosin VIIA tail in co-transfected HEK293 cells. Extracts from co-transfected cells expressing both the myc-tagged A34.2 peptide and the myosin VIIA tail (lane 3) were used for co-immunoprecipitation experiments; the myosin VIIA tail and A34.2 peptide are co-immunoprecipitated with either the anti-myosin VIIA (lane 4) or the anti-myc (lane 5) antibody. When using extracts from HEK293 cells producing the myc-tagged A34.2 peptide alone (lane 1), no immunoprecipitate forms with the anti-myosin VIIA antibody (lane 2). (**C**) Binding of vezatin to the myosin VIIA C-terminal FERM domain. A standard amount of Caco-2 cell lysate containing endogenous vezatin (5% of which is shown in lane SN) was incubated with avidin resins coated with different biotinylated myosin VIIA peptides (bait, amino acids 1752–2215; BdC2, 1752–1931; BdN1, 1896–2215) or a biotinylated control protein, chloramphenicol acetyltransferase (CAT). Vezatin binds to either the bait peptide or the BdN1 fragment containing only the FERM domain, but not to BdC2 lacking the FERM domain or to CAT.

A34.2 and the myosin VIIA tail were co-immunoprecipitated in both cases (Figure 2B). In addition, in *in vitro* binding and pull down experiments a biotinylated A34 peptide (amino acids 336–569) and endogenous vezatin (Figure 2C) bound to the C-terminal myosin VIIA tail fragment corresponding to the original bait, respectively. They also both bound to an N-terminal truncated version of the bait containing only the FERM domain. In contrast, both failed to bind to a truncated C-terminal bait containing only the MyTH4 domain (see Figure 2C for endogenous vezatin). Taken together, these results demonstrate that vezatin specifically interacts with the C-terminal FERM domain of myosin VIIA.

Co-localization of the myosin VIIA tail and vezatin at cell–cell junctions

We analysed the localization of both the myosin VIIA tail and vezatin in epithelial cells (see Materials and methods). In isolated MDCK cells both the myosin VIIA tail and vezatin displayed a cytoplasmic distribution. However, as soon as cell–cell contacts developed the myosin VIIA tail (Figure 3A) was recruited to cell–cell junctions together with vezatin (Figure 3B and C). Triton X-100 treatment of these cells in culture did not affect the myosin VIIA tail (Figure 3D–F) or vezatin (not shown) staining, revealing that the two molecules belong to insoluble protein complexes present at cell–cell contacts. Interestingly, when unpermeabilized MDCK cells were incubated with two antibodies directed against the predicted extracytoplasmic region of vezatin (see Materials and methods) both antibodies labelled the cell surface, demonstrating that vezatin is a transmembrane protein.

Recruitment of vezatin at adherens junctions

Immunofluorescence analysis of mouse tissue sections showed the presence of vezatin in all epithelia tested (i.e. skin, intestine, lung, liver, kidney and pancreas); the bulk of the immunoreactivity was present at cell–cell contacts (Figure 4A–C). Moreover, in all epithelial cell lines cited above vezatin staining was also seen at the cell–cell junctions (not shown). This led us to study in more detail the localization of vezatin during the establishment of cell–cell contacts in MDCK cells. In semi-confluent MDCK cultures we observed a punctate vezatin staining of the plasma membrane at the sites of initial cell–cell contacts, whereas non-contacting membranes were unlabelled (Figure 4D). The membrane labelling was reminiscent of E-cadherin-positive puncta identified as intermediates in adherens junction formation (Yonemura *et al*., 1995; Adams *et al*., 1996, 1998; Angres *et al*., 1996; Vasioukhin *et al*., 2000). Accordingly, double immunolabelling experiments showed that vezatin (Figure 4D) and E-cadherin (Figure 4E) co-localized at these sites (Figure 4F). At cell confluence both vezatin (Figure 4G) and E-cadherin (Figure 4H) were broadly distributed along the adherens junction (Figure 4I and J). In the murine skin, intestine, liver and pancreas epithelia the two proteins also co-localized at adherens junctions (not shown). In contrast, no co-localization of vezatin and desmoglein (a desmosome-specific protein) was detected in the murine skin or intestine nor was any vezatin immunoreactivity detected at the focal adhesion sites of NIH 3T3 fibroblasts (not shown). These results identify vezatin as a ubiquitous protein of adherens junctions.

Interaction of vezatin with the cadherin–catenins complex

We subsequently tested whether vezatin localizes to adherens junctions mediated by different types of cadherins. To this end, we studied the subcellular

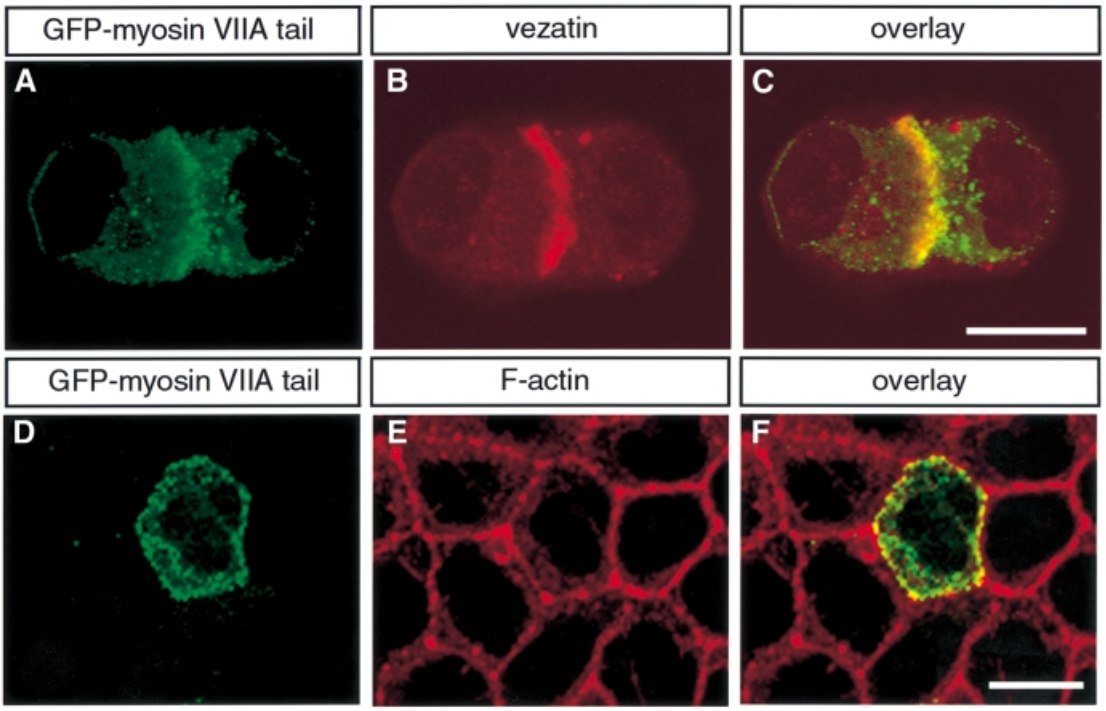

Fig. 3. Co-localization of endogenous vezatin and the myosin VIIA tail fused to GFP in transfected MDCK cells. As soon as cell contacts can be detected, the myosin VIIA tail (**A**) co-localizes with endogenous vezatin (**B**) at the precise membrane sites of the cell–cell contacts (**C**). The same result was obtained with a GFP–myosin VIIA tail fragment composed of the last 464 amino acids of myosin VIIA (not shown). After Triton X-100 treatment the GFP–myosin VIIA tail (**D**) is still associated with the actin complex (**E**) at the cell–cell junctions (**F**). Bar, 10 μm.

distribution of vezatin in L cells and S180 fibroblasts stably transfected with either chicken E-cadherin or N-cadherin (see Materials and methods). In untransfected L (not shown) and S180 cells (Figure 5A), which do not express any known cadherin and do not form cell–cell contacts (Nagafuchi and Takeichi, 1989), vezatin displayed a cytoplasmic distribution. However, the protein was intensively recruited at the contacts established between cells stably transfected with either cadherin (Figure 5B and C). Altogether, these results suggest that vezatin is associated with the cadherin–catenin complex known to play a key role in cell–cell adhesion (Geiger and Ayalon, 1992; Kemler, 1993). Although weak cell–cell adhesion is obtained by a homophilic interaction of the sole cadherin ectodomain, a strong adhesion state is only reached when α-catenin, which links the cadherin–β-catenin complex, binds to the actin cytoskeleton (Nagafuchi and Takeichi, 1988; Ozawa *et al*., 1990; Aberle *et al*., 1994; Stappert and Kemler, 1994; Rimm *et al*., 1995; Yap *et al*., 1997). To test whether vezatin belongs to the cadherin–catenins complex associated with adherens junctions, we performed immunoprecipitation experiments using anti-vezatin antibodies from extracts of MDCK cells, E- or N-cadherin transfected L cells and S180 fibroblasts. Vezatin co-immunoprecipitated with E- or N-cadherin and β- and α-catenins (see Figure 6A).

To analyse further the interaction of vezatin with the cadherin–catenins complex, we took advantage of several stably transfected L cells that express human E-cadherin (L-hEcad) carrying different cytoplasmic deletions (L-hEcadΔ cells) and that still form cell–cell contacts (Lecuit *et al*., 2000). Whereas junctional vezatin labelling was observed in L-hEcad cells (Figure 5D–F), no signal was detected at adherens junctions in L-hEcadΔCyto (Figure 5G–I) and L-hEcadΔCB cells (Figure 5J–L), expressing truncated E-cadherin lacking the cytoplasmic domain (amino acids 582–728) or the β-catenin binding site (amino acids 693–728), respectively. In contrast, vezatin was detected at the junctions of L-hEcadΔPR cells expressing E-cadherin lacking the p120 catenin binding domain (amino acids 582–655) (Figure 5M–O). To determine the relative contribution of the C-terminal region of E-cadherin and of α- and β-catenins to the targeting of vezatin to adherens junctions, we used a chimeric construct in which the E-cadherin transmembrane domain is directly fused to the last 398 C-terminal amino acids of α-catenin (E-cad/α-ctn). A similar chimeric protein has been shown to interact with actin and to support strong cell–cell adhesion (Nagafuchi *et al*., 1994). In E-cad/α-ctn-transfected L cells intense junctional vezatin staining was detected (Figure 5P–R). In addition, using anti-vezatin antibodies α-catenin was co-immunoprecipitated with vezatin from L-hEcadΔCyto and L-hEcadΔCB cell extracts (Figure 6A). A small fraction of β-catenin could be detected in the complex immunoprecipitated with the antibody to vezatin (Figure 6A). This may represent a fraction associated with α-catenin. Having shown that vezatin interacts with the C-terminal region of α-catenin, it was of interest to test whether it simultaneously interacts with myosin VIIA and the E-cadherin–catenin complex. As shown in Figure 6B, using an anti-myosin VIIA antibody the myosin VIIA

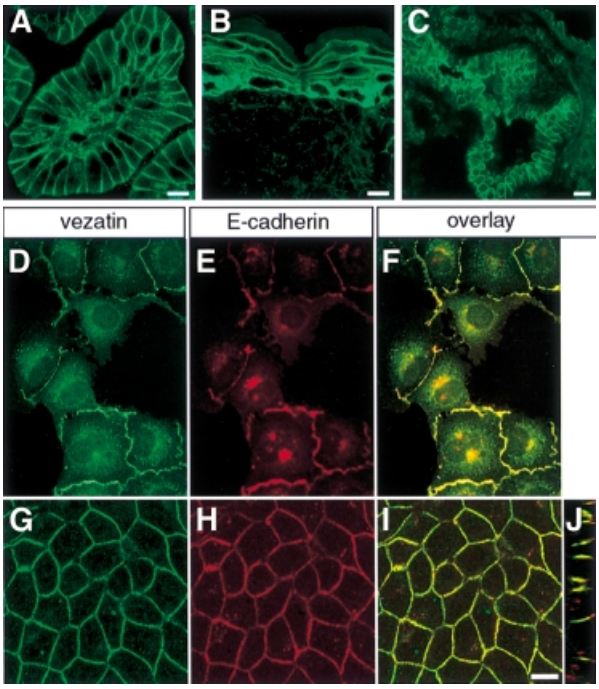

Fig. 4. Vezatin at cell–cell contacts. (**A**–**C**) Expression of vezatin in adult mouse tissues. (A) Oblique section of a P20 mouse intestinal villosity. The vezatin immunoreactivity is mainly localized at the cell–cell junctions of the epithelial cells. The connective tissue is also immunoreactive. (B) P20 mouse skin. The bulk of the vezatin immunoreactivity is located between epidermal cells. A punctate labelling is also detected in the derma. (C) P20 mouse lung. An intense vezatin staining is observed between the epithelial cells of the bronchial tube. (**D**–**J**) Co-localization of vezatin with E-cadherin at cell–cell contacts. MDCK cells were grown to either semi-confluence (D–F) or confluence (G–J). Vezatin (D and G) and E-cadherin (E and H) co-localize at cell–cell contacts (F, I and J). (J) A computer-generated *Z* view (vertical axis) reconstructed from a series of cross-sections, showing the co-distribution of vezatin and E-cadherin along the lateral cell membrane. Co-localizations in the double staining experiments are shown on merged images (F, I and J). Bar, 10 μm.

tail was co-immunoprecipitated along with vezatin, E-cadherin and β- and α-catenins from extracts of myosin VIIA tail-expressing MDCK cells.

Vezatin in the inner ear sensory hair cells

In the inner ear myosin VIIA expression is restricted to the sensory hair cells. It is present throughout the murine hair cells, including the stereocilia (Hasson *et al*., 1995, 1997; El-Amraoui *et al*., 1996), i.e. the stiff actin-filled microvilli forming the mechanoreceptive structure. Based on the strong and locally restricted myosin VIIA immunoreactivity observed in the basal part of the stereocilia in the frog (Hasson *et al*., 1997), a possible association between myosin VIIA and the ankle links, i.e. fibrous structures that interconnect the basal part of the stereocilia (Tilney *et al*., 1988; Goodyear and Richardson, 1999), has been proposed. The distribution of vezatin in the hair cells was studied by immunohistofluorescence, using antibodies directed against either the intra- or extracellular domain of vezatin. A similar labelling pattern was observed with both antibodies. Vezatin was detected at the adherens junctions between the sensory hair and supporting cells. Ultrastructural analysis of the cochlear and vestibular hair cells revealed an intense vezatin labelling at these junctions (Figure 7A), as well as myosin VIIA staining (Figure 7B). In addition, conspicuous vezatin labelling was observed at the base of the hair cell stereocilia (Figure 7C–H), which was shown to face the ankle links by immunoelectron microscopy (Figure 7C). The two following observations indicate that vezatin is tightly associated with the ankle links. In the mouse we observed a post-natal decrease in vezatin immunoreactivity at the base of the stereocilia (almost undetectable at P30) (not shown) that coincided with progressive disappearance of the ankle links (R.Goodyear, personal communication). In contrast, in the chicken, where the ankle links persist throughout life and can be labelled by a monoclonal antibody directed against an ankle link antigen (ALA) (Figure 7L), vezatin immunoreactivity was still present in adult animals (Figure 7K) and co-localized with the ALA labelling (Figure 7M).

Discussion

We report here the identification of a novel transmembrane protein, vezatin, which binds to the C-terminal FERM domain of the unconventional myosin VIIA. Therefore, the FERM domain of myosin VIIA behaves similarly to those of the 4.1 and ERM proteins, which bind to specific membrane proteins allowing their attachment to the plasma membrane (Chishti *et al*., 1998). Several arguments support the conclusion that vezatin anchors myosin VIIA to adherens junctions: (i) myosin VIIA and vezatin co-localize at adherens junctions, as shown by immunoelectron microscopy of inner ear hair cells; (ii) the GFP-tagged myosin VIIA tail is recruited to initial sites of cell–cell contacts in transfected MDCK cells and persists at adherens junctions upon Triton X-100 treatment; (iii) in extracts of these transfected cells the myosin VIIA tail could be co-immunoprecipitated with vezatin and the cadherin–catenins complex using anti-myosin VIIA antibodies. The normal distribution of vezatin in hair cells of the severe myosin VIIA defective *shaker-1* mutant *SB4626* (kindly provided by K.Steel, Nottingham, UK) (data not shown) suggests that the vezatin subcellular distribution is myosin VIIA independent. Based on the present data, we propose that forces generated by myosin VIIA clustered to adherens junctions by its direct and indirect binding to vezatin and cadherin, respectively, increase the tension between the plasma membrane and the actin cytoskeleton. This should have a strengthening effect on the adhesion between adjacent cells. The requirement of a 'myosin activity' to strengthen cell–cell adhesion has recently been postulated (Adams and Nelson, 1998), but has so far only been supported by indirect evidence. In particular, a rodent unconventional myosin, myr 3, has been observed at the cell–cell contacts of cultured fibroblasts (Stöffler *et al*., 1995, 1998) and recently, in pull down assays, cingulin, a protein of the cytoplasmic plaques of tight junctions, was shown to interact with both ZO-1, itself binding to occludin, and with the conventional myosin II (Cordenonsi *et al*., 1999). Therefore, the present results provide a new role for unconventional myosins, i.e in cell–cell adhesion. These motor proteins have previously been shown to be involved in the formation and movement of cellular processes, in vesicle mobility and in signal transduction

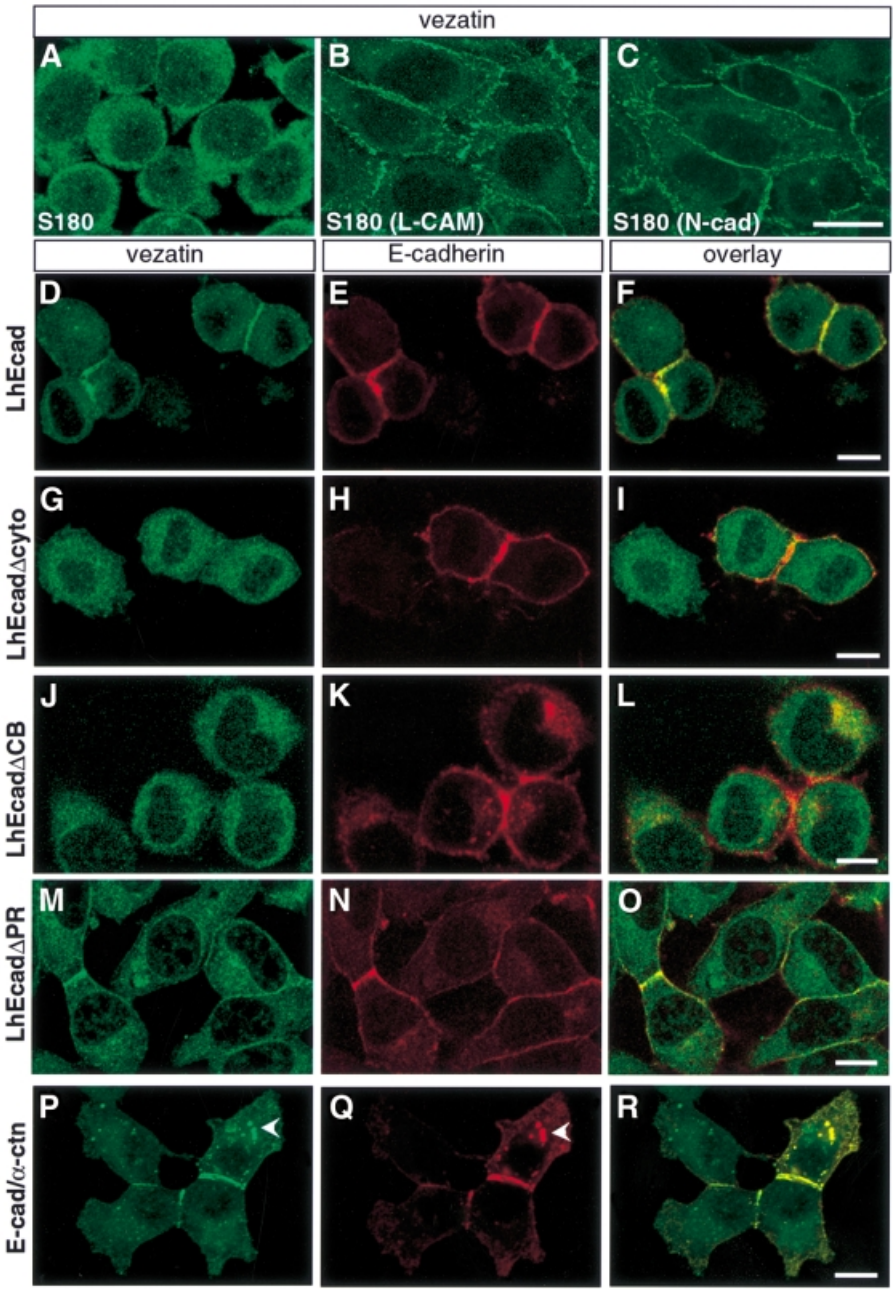

Fig. 5. Vezatin interacts with the cadherin–catenin complex. (**A**–**C**) Localization of vezatin in S180 cells expressing chicken E-cadherin (L-CAM) or N-cadherin (N-cad). In S180 fibroblasts (A), which lack E-cadherin and adherens-like junctions, vezatin is distributed throughout the cytoplasm. In contrast, in stably transfected S180 cells expressing chicken L-CAM (B) or N-cadherin (C) an intense vezatin labelling is detected at cell–cell contacts. (**D**–**R**) Vezatin localization in transfected L2071 cells expressing different truncated E-cadherin (D–O) or E-cadherin–α-catenin chimeras (P–R). In L cells stably transfected with the entire human E-cadherin (L-hEcad), vezatin (D) as well as E-cadherin (E) is recruited to the cell–cell contacts (F). In contrast, in L cells stably expressing hEcad lacking either the cytoplasmic domain (L-hEcadΔCyto) (G–I) or the β-catenin binding domain (L-hEcadΔCB) (J–L) vezatin has a cytoplasmic localization. In L cells expressing hEcad lacking the p120-catenin binding site (L-hEcadΔPR) vezatin is recruited to the cell junction (M–O). In L cells expressing the E-cadherin–α-catenin chimera, linking the E-cadherin transmembrane domain directly to the last 398 C-terminal amino acids of α-catenin, vezatin is detected at the cell–cell junctions (P–R). Note the cytoplasmic localizations of vezatin and E-cadherin–α-catenin chimera (arrowheads). Bar, 10 μm.

(Richardson *et al*., 1997; Mermall *et al*., 1998; Oliver *et al*., 1999; Titus, 1999).

Vezatin at adherens junctions has a double interaction with the actin filaments networks, via the unconventional myosin VIIA and via the cadherin–catenins complex. Our results indicate that vezatin is first recruited to adherens junctions via an interaction with α-catenin and then anchors myosin VIIA to these sites. However, vezatin may simultaneously be involved in the two actin interaction pathways via two distinct binding sites, since anti-myosin VIIA antibody co-immunoprecipitated vezatin, E-cadherin and α- and β-catenin. The role of vezatin in cells that do not express myosin VIIA remains to be elucidated, as it remains to be established whether or not vezatin directly binds to α-catenin. It is noteworthy that both the interaction of vezatin with α-catenin, which is known to

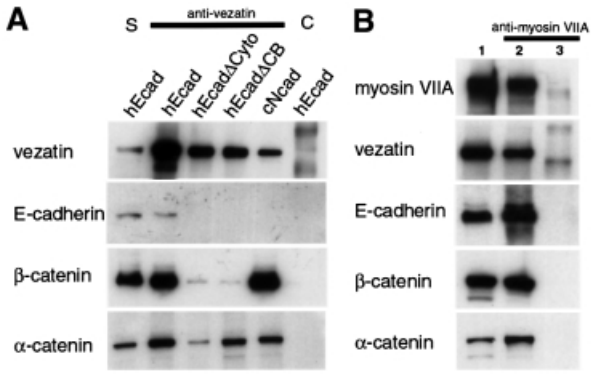

Fig. 6. Immunoprecipitation experiments in transfected cells expressing different forms of E-cadherin. (**A**) Extracts from L cells expressing the entire human E-cadherin (hEcad), human E-cadherin lacking the cytodomain (hEcadΔCyto) or the β-catenin binding domain (hEcadΔCB) and from S180 cells expressing the entire chicken N-cadherin (cNcad) were used. Vezatin, α-catenin and β-catenin are co-immunoprecipitated by an anti-vezatin antibody in cells transfected with either E- or N-cadherin cDNAs. In addition, vezatin and α-catenin are co-immunoprecipitated in cells producing the truncated E-cadherin variants (lanes hEcadΔCyto and hEcadΔCB), whereas only a very small fraction of β-catenin, compared with control (hEcad), is detected in the immunoprecipitate. The preimmune serum (lane C) was used as a negative control. S, soluble fraction. (**B**) In extracts from HEK293 cells expressing myosin VIIA tail (lane 2) the myosin VIIA tail co-immunoprecipitates with vezatin, E-cadherin, β-catenin and α-catenin, using an anti-myosin VIIA antibody. No immunoprecipitation was observed with extracts from non-transfected cells (lane 3). Lane 1 contains the soluble fraction.

play a key role in the establishment of strong cell–cell adhesion (Aberle *et al*., 1994; Rimm *et al*., 1995), and its ubiquitous expression qualify this molecule as a possible important contributor to the formation and maintenance of adherens junctions.

In murine inner ear sensory hair cells vezatin is present at adherens junctions with supporting cells. Vezatin is also concentrated in another site of membrane–membrane interaction, namely at the attachment sites of a subset of lateral links, the ankle links, interconnecting the bases of the stereocilia. These links form concomitantly with the emergence of the stereocilia from the apical cell surface (Tilney *et al*., 1988). Further characterization of the extracellular region of vezatin should clarify whether vezatin makes up the ankle link or is tightly associated with it. In addition, since myosin VIIA is present all along the stereocilia, at least in mammals, it is likely that this myosin interacts, via an as yet unidentified protein, with the other lateral links of the stereocilia. Direct interaction of the myosin VIIA tail with vezatin at the ankle links attachment sites suggests that a tension force is applied to these structures, which should no longer be viewed as inert links between stereocilia. According to the proposed dynamic role of the vezatin–myosin VIIA interaction, this interaction at the base of the stereocilia should contribute to the cohesion of the hair bundle during development of the stereocilia. Moreover, a possible role for the vezatin–myosin VIIA interaction at adherens junctions on the orientation of the stereocilia should also be considered. Indeed, the resulting stabilization of adherens junctions could in turn stabilize the dense meshwork of apical horizontal filaments (the cuticular plate) (Slepecky, 1996; Eaton, 1997), which is linked to the actin filament rootlets of the stereocilia (Hirokawa and Tilney, 1982). Therefore, we suggest that the interaction of vezatin with myosin VIIA fully accounts for the splaying out of hair cell stereocilia, which characterizes the sensory hair cells of myosin VIIA-defective mutants.

In conclusion, by searching for a ligand of myosin VIIA, we identified a protein corresponding to what had long been the missing link between the E-cadherin–catenin–actin junctional complex and the actinomyosin-based contractile system (Adams and Nelson, 1998). We anticipate that vezatin plays a pivotal role in the establishment of adherens junctions and their maintenance in adult life.

Materials and methods

Sequence analysis

To isolate the A34 cDNA, a human retinal cDNA library in λgt11 (Clontech) was screened. Sequence analysis revealed four overlapping cDNAs designated A34.1, A34.2, A34.4 and A34.6 (see Figure 1). The 5′-RACE–PCR performed to extend the A34 sequence resulted in two amplification products, A34.3 and A34.5 (Figure 1). A search with the A34.1 sequence as a query in the EST databases, using the BLAST 2.0 algorithm, identified >100 human ESTs, covering almost the entire length of A34.1, and 12 murine ESTs showing 80–90% nucleotide identity with the human sequence. The longest EST clones were completely sequenced; however, none of them extended beyond the GC-rich 5′-region of A34.4. Sequence comparison of the cDNA and EST clones with available genome sequences revealed multiple splice variants differing in their extra- or intracellular regions. Seven alternative splicing sites in the cytoplasmic domain and six in the extracellular region were identified (see Figure 1).

The helical transmembrane segment present in some of these isoforms was predicted by the PHDhtm (Rost *et al*., 1995) (http://www.heidelberg.de/Services/index.html) and PSORT II (http://psort.nibb.ac.jp) programs.

Antibody production

Different rabbit polyclonal anti-vezatin antibodies were generated: anti-mA34 was raised against a His_6-tagged A34 murine protein derived from EST W33426 (mA34, orthologous to amino acids 317–568 of A34.1); anti-hA34P1 and anti-hA34P2 were directed against two epitopes in the extracytoplasmic domain of human vezatin (see Figure 1), hA34P1 (CFENSPLYQYLQDLGH) and hA34P2 (CTTEGQQKPPTRVLPK), respectively. The specificity of the immunopurified antibodies was checked by immunoblot and immunofluorescence analyses. The anti-mA34 antibody detected a sole band on cell extracts expressing the human myc-tagged A34.2 protein. All antibodies, anti-mA34, anti-hA34P1 and anti-hA34P2, gave the same distribution patterns in inner ear hair cells and MDCK cells. Substitution of preimmune sera for the purified anti-vezatin antibodies and pre-adsorption of the antibodies with the corresponding antigen were used as negative controls.

Immunoprecipitation, in vitro binding and pull down experiments

The myosin VIIA tail (amino acids 848–2215) was reconstituted from several cDNAs by PCR and restriction enzyme site cloning (Küssel-Andermann *et al*., 2000). Transient transfections were performed using Lipofectamine Plus (Gibco) following the manufacturer's protocol. Cells were collected 1–2 days after transfection and processed as described (Küssel-Andermann *et al*., 2000). To produce the myosin VIIA biotinylated fusion proteins, i.e. the bait and its truncated forms, the following constructs were generated in PinPoint Xa (pXa) vectors (Promega): pXa1-bait (amino acids 1752–2215), pXa1-BdC2 (amino acids 1752–1931) and pXa2-BdN1 (amino acids 1896–2215). Bacteria containing the biotinylated A34 peptide (amino acids 336–569 of A34.1) or Caco-2 cells expressing endogenous vezatin were lysed in binding buffer (50 mM Tris–HCl pH 7.5, 150 mM NaCl, 5 mM $MgCl_2$, 1 mM EDTA, 10% glycerol, 0.5% NP-40) supplemented with a mixture of proteinase inhibitors. Immunoprecipitation and *in vitro* binding were

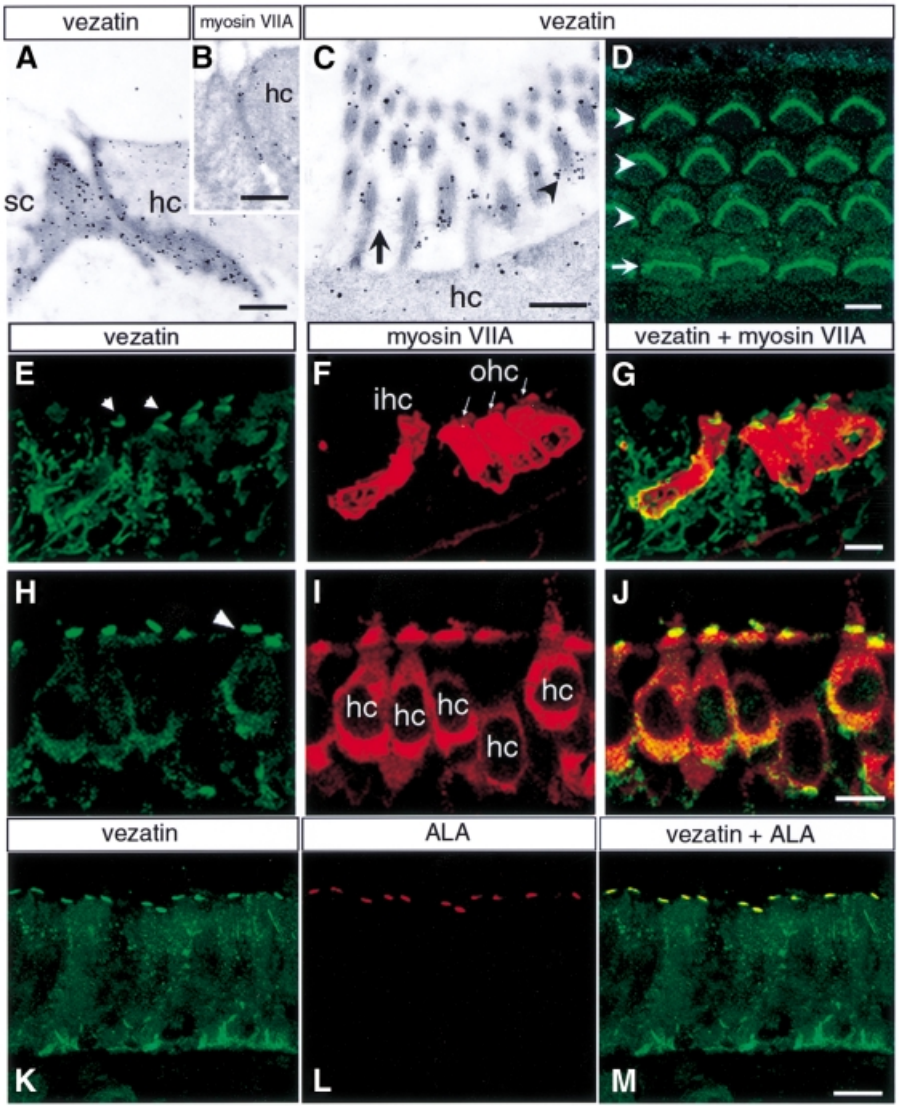

Fig. 7. Co-localization of vezatin, myosin VIIA and the ankle link antigen (ALA) in the inner ear. (**A**–**C**) Immunoelectron microscopy of the mouse cochlea, showing the ultrastructural distribution of vezatin and myosin VIIA. (A and B) Oblique sections through the junction between a hair cell (hc) and a supporting cell (sc) at P30, showing vezatin (A) and myosin VIIA (B) labelling along the adherens junction. (C) In the hair bundle vezatin labelling is concentrated at the base (arrowhead) of the stereocilia, where the ankle links (arrow) are located. (**D**–**M**) Immunohistofluorescence. (D) Whole mount preparation of a P2 organ of Corti. Vezatin immunoreactivity is observed in the stereocilia hair bundles of the three rows (arrowheads) of outer hair cells (W shape) and the single row (arrow) of inner hair cells (U shape). (E–G) P2 mouse cochlea (fixed with PFA). (E) Vezatin is detected in the inner (ihc) and outer (ohc) hair cells of the organ of Corti. Note that the hair bundles are strongly immunoreactive (arrowheads). Vezatin is also detected in the supporting cells and nerve fibres. When either unfixed or methanol fixed sections were used a strong vezatin labelling was observed also at the cell–cell contacts between hair cells and supporting cells (not shown). (F) Myosin VIIA is restricted to the ihc and ohc, where it is localized throughout the cell. (H–J) P8 mouse utricular hair cells (hc). (H) The strongest vezatin immunoreactivity is at the base of the stereocilia (arrowhead), whereas the myosin VIIA labelling (I) appears more uniform. (K–M) Adult chicken inner ear macula. Vezatin (K) and the ankle link antigen ALA (L) are co-localized (M) at the base of the stereocilia. Bars: (A) and (B) 0.1 μm; (C) 0.5 μm; (D)–(M) 10 μm.

performed as previously described (Küssel-Andermann *et al*., 2000). For pull down experiments, after coating of avidin resin (Promega) with a biotinylated myosin VIIA peptide (see above) or the biotinylated control protein (CAT), possible free avidin molecules were blocked by post-incubation with 5 mM biotin. The coated resin was then incubated for 2 h at 4°C with the protein cell extracts. The resin was washed five times and bound proteins were separated by SDS–PAGE and analysed by immunobloting, using either a streptavidin–horseradish peroxidase (HRP) conjugate or the anti-mA34 antibody followed by an HRP-conjugated goat anti-rabbit IgG.

Cell lines and antibodies

All cell lines (MDCK, LLCPK, Caco-2, HEK293, HeLa, NIH 3T3, L and S180) were maintained in Dulbecco's modified Eagle's medium supplemented with 10% fetal bovine serum (Gibco BRL) and antibiotics in 6% CO_2. G418 (800 μg/ml) was added to the culture medium for stably transfected L cells.

Different mouse fibroblast cell lines were used: S180, S180 stably expressing either chicken E-cadherin, LCAM (2B2) or N-cadherin (ARM); L2071, L2071 stably expressing either entire human E-cadherin (L-hEcad) or different truncated variants (Lecuit *et al*., 2000), L-hEcadΔCyto (which lacks the entire hEcad cytoplasmic domain), L-hEcadΔCB (lacking the last 35 amino acids of the hEcad cytoplasmic domain) and L-hEcadΔPR (without the p120-catenin binding domain). A chimeric construct (E-cad/α-ctn), resulting from fusion of the hEcad transmembrane domain (amino acids 1–580) with the C-terminal 398 amino acids of mouse α-catenin (Lecuit *et al*., 2000), was used for transient transfections. All the cell lines were fixed with cold methanol for 5 min at –20°C and handled for immunofluorescence as previously described (El-Amraoui *et al*., 1996).

The anti-E-cadherin (DECMA-1) antibody was a gift from M.Arpin (Institut Curie, Paris, France). A mouse anti-human E-cadherin (HECD1) antibody directed against the ectodomain was provided by M.Takeichi (Shimoyama *et al*., 1989). The anti-α-/β- and p120-catenin antibodies were from Transduction Laboratories. The ankle links were detected with the ALA antibody kindly provided by G.Richardson (Brighton, UK). For vezatin–myosin VIIA double labelling experiments a polyclonal mouse antibody raised against a human myosin VIIA tail fragment (amino acids 905–1032) was used. For immunoelectron microscopic detection of myosin VIIA antibodies raised against the amino acids 941–1071 fragment of mouse myosin VIIA were employed (Liu *et al*., 1997; Wolfrum *et al*., 1998).

Immunofluorescence and electron microscopy analysis

For immunofluorescence mouse tissues and inner ears were fixed and treated as previously described (El-Amraoui *et al*., 1996; Sahly *et al*., 1997). For whole mount preparations of the organ of Corti mouse inner ears were fixed and decalcified, then half turns of the cochlea were carefully dissected to separate the organ of Corti and immediate surrounding tissues. Tissue sections or the whole organ of Corti were used for indirect immunofluorescence (El-Amraoui *et al*., 1996). Triton X-100 treatment was performed in cytoskeleton buffer (CSK) (10 mM PIPES pH 6.8, 50 mM NaCl, 3 mM $MgCl_2$, 300 mM sucrose, 1 mM phenylmethylsulfonyl fluoride, 0.5% Triton X-100, 100 μg RNase, 100 μg DNase). Fixation was performed with either 4% paraformaldehyde (PFA) in phosphate-buffered saline or methanol. Cells and tissues sections were analysed on a conventional epifluorescent microscope (Leica) or a laser scanning confocal microscope (LSM-540; Zeiss).

Immunoelectron microscopy was performed on LR White embedded ultra-thin sections of the mouse inner ear (C3H strain), as previously described (Wolfrum *et al*., 1998; Wolfrum and Schmitt, 2000). Nanogold (Nanoprobes, Stony Brook, NY) labelling of ultra-thin sections was silver enhanced as described (Danscher, 1981) and analysed on a Zeiss EM900 or Zeiss EM912Ω electron microscope.

Acknowledgements

We thank Jean-Pierre Hardelin, Monique Arpin, Michel Bornens and Olivier Ardouin for helpful discussions and critical reading of the manuscript and Jacqueline Levilliers and Dominique Weil for their continuous and inexhaustible help. This work was supported by grants from the EC (QLG2-CT-1999-00988), Retina-France, A. & M. Suchert and Forschung contra Blindheit-Initiative Usher Syndrome, a C. & J.-P. Bernais donation, Deutsche Forschungsgemeinschaft (Wo 548/3-1/2 and Wo 548/4-1) (U.W.), FAUN-Stiftung, Nürnberg (U.W.) and the Pasteur Weizmann Joint Research Program (P.C.).

References

Aberle,H., Butz,S., Stappert,J., Weissig,H., Kemler,R. and Hoschuetzky,H. (1994) Assembly of the cadherin-catenin complex *in vitro* with recombinant proteins. *J. Cell Sci.*, **107**, 3655–3663.

Adams,C.L. and Nelson,W.J. (1998) Cytomechanics of cadherin-mediated cell–cell adhesion. *Curr. Opin. Cell Biol.*, **10**, 572–577.

Adams,C.L., Nelson,W.J. and Smith,S.J. (1996) Quantitative analysis of cadherin-catenin–actin reorganization during development of cell–cell adhesion. *J. Cell Biol.*, **135**, 1899–1911.

Adams,C.L., Chen,Y.T., Smith,S.J. and Nelson,W.J. (1998) Mechanisms of epithelial cell–cell adhesion and cell compaction revealed by high-resolution tracking of E-cadherin–green fluorescent protein. *J. Cell Biol.*, **142**, 1105–1119.

Angres,B., Barth,A. and Nelson,W.J. (1996) Mechanism for transition from initial to stable cell–cell adhesion: kinetic analysis of E-cadherin-mediated adhesion using a quantitative adhesion assay. *J. Cell Biol.*, **134**, 549–557.

Avraham,K.B., Hasson,T., Steel,K.P., Kingsley,D.M., Russell,L.B., Mooseker,M.S., Copeland,N.G. and Jenkins,N.A. (1995) The mouse *Snell's waltzer* deafness gene encodes an unconventional myosin required for structural integrity of inner ear hair cells. *Nature Genet.*, **11**, 369–375.

Chen,Z.-Y., Hasson,T., Kelley,P.M., Schwender,B.J., Schwartz,M.F., Ramakrishnan,M., Kimberling,W.J., Mooseker,M.S. and Corey,D.P. (1996) Molecular cloning and domain structure of human myosin-VIIa, the gene product defective in Usher syndrome 1B. *Genomics*, **36**, 440–448.

Chishti,A.H. *et al*. (1998) The FERM domain: a unique module involved in the linkage of cytoplasmic proteins to the membrane. *Trends Biochem. Sci.*, **23**, 281–282.

Cordenonsi,M., D'Atri,F., Hammar,E., Parry,D.A.D., Kendrick-Jones,J., Shore,D. and Citi,S. (1999) Cingulin contains globular and coiled-coil domains and interacts with ZO-1, ZO-2, ZO-3 and myosin. *J. Cell Biol.*, **147**, 1569–1582.

Danscher,G. (1981) Localization of gold in biological tissue. A photochemical method for light and electronmicroscopy. *Histochemistry*, **71**, 81–88.

Eaton,S. (1997) Planar polarization of drosophila and vertebrates epithelia. *Curr. Opin. Cell Biol.*, **9**, 860–866.

El-Amraoui,A., Sahly,I., Picaud,S., Sahel,J., Abitbol,M. and Petit,C. (1996) Human Usher IB/mouse *shaker-1*; the retinal phenotype discrepancy explained by the presence/absence of myosin VIIA in the photoreceptor cells. *Hum. Mol. Genet.*, **5**, 1171–1178.

Ernest,S., Rauch,G.-J., Hafter,P., Geisler,R., Petit,C. and Nicolson,T. (2000) Mariner is defective in myosin VIIA: a zebrafish model for human hereditary deafness. *Hum. Mol. Genet.*, **9**, 2189–2196.

Geiger,B. and Ayalon,O. (1992) Cadherins. *Annu. Rev. Cell Biol.*, **8**, 307–332.

Gibson,F., Walsh,J., Mburu,P., Varela,A., Brown,K.A., Antonio,M., Beizel,K.W., Steel,K.P. and Brown,S.D.M. (1995) A type VII myosin encoded by the mouse deafness gene *Shaker-1*. *Nature*, **374**, 62–64.

Goodyear,R. and Richardson,G. (1999) The ankle-link antigen: an epitope sensitive to calcium chelation associated with the hair-cell surface and the calycal processes of photoreceptors. *J. Neurosci.*, **19**, 3761–3772.

Hasson,T., Heintzelman,M.B., Santos-Sacchi,J., Corey,D.P. and Mooseker,M.S. (1995) Expression in cochlea and retina of myosin VIIa, the gene product defective in Usher syndrome type 1B. *Proc. Natl Acad. Sci. USA*, **92**, 9815–9819.

Hasson,T., Gillespie,P.G., Garcia,J.A., MacDonald,R.B., Zhao,Y., Yee,A.G., Mooseker,M.S. and Corey,D.P. (1997) Unconventional myosins in inner-ear sensory epithelia. *J. Cell Biol.*, **137**, 1287–1307.

Hirokawa,N. and Tilney,L.G. (1982) Interactions between actin filaments and between actin filaments and membranes in quick-frozen and deeply etched hair cells of the chick ear. *J. Cell Biol.*, **95**, 249–261.

Hoyt,M.A., Hyman,A.A. and Bahler,M. (1997) Motor proteins of the eukaryotic cytoskeleton. *Proc. Natl Acad. Sci. USA*, **94**, 12747–12748.

Kemler,R. (1993) From cadherins to catenins: cytoplasmic protein interactions and regulation of cell adhesion. *Trends Genet.*, **9**, 317–321.

Küssel-Andermann,P., El-Amraoui,A., Safieddine,S., Hardelin,P., Nouaille,S., Camonis,J. and Petit,C. (2000) Unconventional myosin VIIA is a novel A-kinase anchoring protein. *J. Biol. Chem.*, **275**, 29654–29659.

Lecuit,M., Hurme,R., Pizarro-Cerdà,J., Ohayon,H., Geiger,B. and Cossart,P. (2000) A role for α- and β-catenins in bacterial uptake. *Proc. Natl Acad. Sci. USA*, **97**, 10008–10013.

Liu,X., Vansant,G., Udovichenko,I.P., Wolfrum,U. and Williams,D.S. (1997) Myosin VIIa, the product of the Usher 1B syndrome gene, is concentrated in the connecting cilia of photoreceptor cells. *Cell Motil. Cytoskeleton*, **37**, 240–252.

Liu,X.R., Ondek,B. and Williams,D.S. (1998) Mutant myosin VIIA causes defective melanosome distribution in the RPE of *shaker-1* mice. *Nature Genet.*, **19**, 117–118.

Liu,X.R., Udovichenko,I.P., Brown,S.D., Steel,K.P. and Williams,D.S. (1999) Myosin VIIA participates in opsin transport through the photoreceptor cilium. *J. Neurosci.*, **19**, 6267–6274.

Mermall,V., Post,P.L. and Mooseker,M.S. (1998) Unconventional myosins in cell movement, membrane traffic and signal transduction. *Science*, **279**, 527–533.

Nagafuchi,A. and Takeichi,M. (1988) Cell binding function of E-cadherin is regulated by the cytoplasmic domain. *EMBO J.*, **7**, 3679–3684.

Nagafuchi,A. and Takeichi,M. (1989) Transmembrane control of cadherin-mediated cell adhesion: a 94 kDa protein functionally associated with a specific region of the cytoplasmic domain of E-cadherin. *Cell Regul.*, **1**, 37–44.

Nagafuchi,A., Ishihara,S. and Tsukita,S. (1994) The roles of catenins in the cadherin-mediated cell adhesion: functional analysis of E-cadherin–α catenin fusion molecules. *J. Cell Biol.*, **127**, 235–245.

Oliver,T.N., Berg,J.S. and Cheney,R.E. (1999) Tails of unconventional myosins. *Cell. Mol. Life Sci.*, **56**, 243–257.

Ozawa,M., Ringwald,M. and Kemler,R. (1990) Uvomorulin–catenin complex formation is regulated by a specific domain in the cytoplasmic region of the cell adhesion molecule. *Proc. Natl Acad. Sci. USA*, **87**, 4246–4250.

Probst,F.J. *et al*. (1998) Correction of deafness in *shaker-2* mice by an unconventional myosin in a BAC transgene. *Science*, **280**, 1444–1447.

Richardson,G.P., Forge,A., Kros,C.J., Fleming,J., Brown,S.D. and Steel,K.P. (1997) Myosin VIIA is required for aminoglycoside accumulation in cochlear hair cells. *J. Neurosci.*, **17**, 9506–9519.

Rimm,D.L., Koslov,E.R., Kebriaei,P., Cianci,C.D. and Morrow,J.S. (1995) α1(E)-catenin is an actin-binding and -bundling protein mediating the attachment of F-actin to the membrane adhesion complex. *Proc. Natl Acad. Sci. USA*, **92**, 8813–8817.

Rost,B., Casadio,R., Farizelli,P. and Sander,C. (1995) Prediction of helical transmembrane segments at 95% accuracy. *Protein Sci.*, **4**, 521–533.

Sahly,I., El-Amraoui,A., Abitbol,M., Petit,C. and Dufier,J.-L. (1997) Expression of myosin VIIA during mouse embryogenesis. *Anat. Embryol.*, **196**, 159–170.

Self,T., Mahony,M., Fleming,J., Walsh,J., Brown,S.D.M. and Steel,K.P. (1998) Shaker-1 mutations reveal roles for myosin VIIA in both development and function of cochlear hair cells. *Development*, **125**, 557–566.

Shimoyama,Y., Hirohashi,S., Hirano,S., Noguchi,M., Shimosato,Y., Takeichi,M. and Abe,O. (1989) Cadherin cell-adhesion molecules in human epithelial tissues and carcinomas. *Cancer Res.*, **49**, 2128–2133.

Slepecky,N.B. (1996) Structure of the mammalian cochlea. In Dallos,P., Popper,A.N. and Fay,R.R. (eds), *The Cochlea*. Springer-Verlag, New York, NY, pp. 44–129.

Stappert,J. and Kemler,R. (1994) A short core region of E-cadherin is essential for catenin binding and is highly phosphorylated. *Cell Adhesion Commun.*, **2**, 319–327.

Stöffler,H.E., Ruppert,C., Reinhard,J. and Bähler,M. (1995) A novel mammalian myosin I from rat with an SH3 domain localizes to Con A-inducible, F-actin-rich structures at cell–cell contacts. *J. Cell Biol.*, **129**, 819–830.

Stöffler,H.E., Honnert,U., Bauer,C.A., Hofer,D., Schwarz,H., Muller,R.T., Drenckhahn,D. and Bahler,M. (1998) Targeting of the myosin-I myr 3 to intercellular adherens type junctions induced by dominant active Cdc42 in HeLa cells. *J. Cell Sci.*, **111**, 2779–2788.

Tilney,L.G., Tilney,M.S. and Cotanche,D.A. (1988) Actin filaments, stereocilia and hair cells of the bird cochlea. V. How the staircase pattern of stereociliary lengths is generated. *J. Cell Biol.*, **106**, 355–365.

Titus,M.A. (1999) A class VII unconventional myosin is required for phagocytosis. *Curr. Biol.*, **9**, 1297–1303.

Vasioukhin,V., Bauer,C., Yin,M. and Fuchs,E. (2000) Directed actin polymerization is the driving force for epithelial cell–cell adhesion. *Cell*, **100**, 209–219.

von Heijne,G. and Gavel,Y. (1988) Topogenic signals in integral membrane proteins. *Eur. J. Biochem.*, **174**, 671–678.

Wang,A. *et al*. (1998) Association of unconventional myosin *MYO15* mutations with human nonsyndromic deafness *DFNB3*. *Science*, **280**, 1447–1451.

Weil,D. *et al*. (1995) Defective myosin VIIA gene responsible for Usher syndrome type 1B. *Nature*, **374**, 60–61.

Weil,D., Küssel,P., Blanchard,S., Lévy,G., Levi-Acobas,F., Drira,M., Ayadi,H. and Petit,C. (1997) The autosomal recessive isolated deafness, DFNB2 and the Usher 1B syndrome are allelic defects of the myosin-VIIA gene. *Nature Genet.*, **16**, 191–193.

Wolfrum,U. and Schmitt,A. (2000) Rhodopsin transport in the membrane of the connecting cilium of mammalian photoreceptor cells. *Cell Motil. Cytoskeleton*, **46**, 95–107.

Wolfrum,U., Liu,X., Schmitt,A., Udovichenko,I.P. and Williams,D.S. (1998) Myosin VIIa as a common component of cilia and microvilli. *Cell Motil. Cytoskeleton*, **40**, 261–271.

Yap,A.S., Brieher,W.M. and Gumbiner,B.M. (1997) Molecular and functional analysis of cadherin-based adherens junctions. *Annu. Rev. Cell Dev. Biol.*, **13**, 119–146.

Yonemura,S., Itoh,M., Nagafuchi,A. and Tsukita,S. (1995) Cell-to-cell adherens junction formation and actin filament organization: similarities and differences between non-polarized fibroblasts and polarized epithelial cells. *J. Cell Sci.*, **108**, 127–142.

Received July 26, 2000; revised and accepted September 25, 2000